Journal of Molecular Catalysis A: Chemical 309 (2009) 71–78

Contents lists available at ScienceDirect

Journal of Molecular Catalysis A: Chemical

journal homepage: www.elsevier.com/locate/molcata

Acidic catalysts for the dehydration of glycerol: Activity and deactivation

Wladimir Suprun*, Michal Lutecki, Thomas Haber, Helmut Papp

Institute of Industrial Chemistry, University of Leipzig, Linnéstraße 3, D-04103 Leipzig, Germany

ARTICLE INFO

Article history:
Received 30 March 2009
Received in revised form 22 April 2009
Accepted 23 April 2009
Available online 3 May 2009

Keywords:
Glycerol
Dehydration
Acrolein
Catalysis
Gas phase
Deactivation

ABSTRACT

Al_2O_3 and TiO_2 supports modified by impregnation with PO_4-ions and SAPO-11 and SAPO-34 samples were synthesized and characterized by physico-chemical methods. The acidic properties of these catalysts were determined by ammonia TPD. The gas-phase dehydration of glycerol in presence of water was investigated at 280 °C. Glycerol conversion and acrolein selectivity depended on the total acidity and on the textural properties. Additionally, the formation of by-products during the dehydration of glycerol and the conversion of 1-hydroxyacetone and 3-hydroxypropionaldehyde catalysts was studied. The SAPO samples showed high selectivity at low reaction times. Rapid deactivation and formation of carbonaceous deposits was observed for all tested catalysts. The properties of the deactivated catalysts were studied by TPD-NH_3 and TPO analysis.

1. Introduction

In recent years, the increasing production of biodiesel has resulted in a price decline of crude glycerol, making aqueous glycerol an attractive compound for the synthesis of fine and crude chemicals [1]. The conversion of glycerol to acrolein opened a new route for the production of acrylate monomers from renewable raw materials. Various solid acid catalysts including sulfates, phosphates, zeolites, supported heteropolyacids have been tested for the dehydration of glycerol in the gas phase [2–6]. Raw glycerol is usually containing water. The direct use of raw glycerol containing water without water removal would be an advantage for the production of acrolein. Therefore, a high water tolerance and long life time of acidic catalysts is necessary for this process. The dehydration of glycerol in gas phase on acidic catalysts proceeds via the formation of 3-hydroxypropionaldehyde (3-HPA) and 1-hydroxyacetone (acetol) [7]. The highest selectivity to acrolein reported was 65–80%. It was found [2–6] that solids acid with a Hammet acidity Ho between −10 and −16 are more suitable for the dehydration of glycerol to acrolein than catalysts of lower acidity with Ho between −2 and −6. Catalysts with an acidity of Ho between −3 and −10 can be chosen from natural or synthetic siliceous materials, from acidic zeolites and from mineral supports (TiO_2, Al_2O_3 and ZrO_2) impregnated with acidic functions such as sulphate, phosphate, tungstate, molybdate or alternatively heteropolyacids. The biggest disadvantage of these catalysts lies in the formation of a large amount of by-products (25–40%) and a progressive catalyst deactivation [5,8,9]. In order to understand the deactivation mechanism during the dehydration of glycerol, we investigated the catalytic activity of supported phosphates (Al_2O_3–PO_4, TiO_2–PO_4) and selected SAPO samples. Additionally, the dehydration of 3-HPA and acetol on these catalysts in presence of water, as well as the deactivation of the catalysts was studied.

2. Experimental

2.1. Catalyst preparation

Al_2O_3–PO_4 and TiO_2–PO_4 with 10 wt% PO_4 were prepared by impregnation, using a 15 wt% H_3PO_4 solution and as supports χ-Al_2O_3, from Aldrich and TiO_2–Anatas, from Millenium GmbH respectively [10]. The impregnated Al_2O_3–PO_4, TiO_2–PO_4 precursors were dried at 120 °C for 12 h. Subsequently, the compounds were calcined in nitrogen at 530 °C for 3 h. Finally, the catalysts were crushed to particles between 100 and 300 μm. SAPO-34 and SAPO-11 were prepared by Süd-Chemie GmbH (Bitterfeld, Germany) following the procedure described by Lok et al. [11]. Prior to use, the samples were calcined for 5 h at 530 °C in a dry air stream.

2.2. Characterization techniques

The catalysts were characterized by textural analysis, X-ray diffraction, and thermal analysis (TPD-NH_3, TPO). BET surfaces, pore volumes and average pore diameters of fresh and of used samples were determined by nitrogen adsorption using a Micrometrics ASAP 2020 apparatus. The crystalline structure of the samples was

* Corresponding author. Tel.: +49 341 9736300; fax: +49 341 9736349.
E-mail address: suprun@chemie.uni-leipzig.de (W. Suprun).

1381-1169/$ – see front matter © 2009 Elsevier B.V. All rights reserved.
doi:10.1016/j.molcata.2009.04.017

determined by powder X-ray diffraction (XRD) using a Bruker D8 Advance X-ray diffractometer with Cu K_α at 40 kV and 40 μA.

The acidity of the fresh and the used catalysts was measured by temperature-programmed desorption of ammonia. Prior to monitoring of the TPD-NH_3 profiles, the samples were heated in a helium flow at 300 °C for 1 h. After cooling to 90 °C, the samples were exposed to ammonia and flushed with a 50 ml/min helium flow for 60 min. The TPD measurements were carried out with a heating rate of 10 K/min up to 600 °C under flowing helium (50 ml/min). The desorption of ammonia (*m*/*e*: 16) were monitored with a MS detector (GSD 301, Pfeiffer Vacuum). The amount of desorbed ammonia was quantified with the help of a reference test, using a defined ammonia pulse over 50 mg of inert quartz.

The deposits of carbon on the used catalysts were measured by temperature programmed oxidation using a thermo gravimetric instrument STA-409 (Fa. Netzsch), coupled with a MS-Analyser (GSD 301; Pfeiffer Vacuum). The TPO experiments were carried out starting from room temperature up to 700 °C with a heating rate of 10 K/min in an air flow of 75 ml/min. The amount of carbon dioxide (*m*/*e*: 44) formed during the combustion of coke was quantified by the thermal decomposition of $CaCO_3$.

2.3. Catalytic test reaction

The catalytic dehydration of glycerol and the catalytic conversion of acetol and 3-HPA were performed at atmospheric pressure in a fixed-bed reactor. Glycerol and acetol were obtained from Merck. 3-HPA was synthesized by the hydration of acrolein in the presence of Dowex 50 WX4-200 (cation exchange material) according to Hall and Stern [12]. Prior to the catalytic reaction a mixture of 200 mg catalyst and 200 mg inert quartz was pre-treated for 15 h in a helium flow of 5 l/h in the presence of 15 vol% water at 320 °C. After cooling to 280 °C, the catalytic setup was run for 1 h to establish steady state conditions. The amount of the aqueous solution of the reactants (mass concentration 5%) was adjusted with liquid flow controllers (500 mg/h) and evaporated at 200 °C in an evaporator (Controller Evaporator Mixer; Type: W101-910P; Bronkhorst High Tech) entering the reactor in down-flow mode. The performance of the catalyst was normally measured at 280 °C with a GHSV of glycerol, 3-HPA and acetol of 43 and 90 h^{-1}.

In order to quantify the reaction products obtained during the reaction, the reaction mixture was collected after 1 or 2 h on stream by condensation in an ice-water trap and analysed by GC-Analysis. The water sample was analysed without preliminary separation using a gas chromatograph (Chrompack 9001) equipped with a capillary column (30 m, ID: 0.32 mm, MACHERY-NAGEL) and a FID detector, TP: 100 °C (2 min isotherm), 12 K/min, 245 °C (5 min isotherm). Quantification was realised by mixing 500 μl of non-diluted reaction mixture with 500 μl of a 3 wt% water solution of ethylene glycol as internal standard. Glycerol conversion (X) and product selectivity (S_i) were calculated according to the following equations [6]:

$$X\,(\text{mol\%}) = \frac{n_{Gl}\,input - n_{Gl}\,output}{n_{Gl}\,input} \times 100$$

$$S_i\,(\text{mol\%}) = \frac{ni}{n\,Feed, o - n\,Feed} \times \frac{zi}{z\,Feed} \times 100$$

where: n_{Gl} *input* and n_{Gl} *output* are the molar streams of glycerol at the input and output; *ni* molar stream of product; (*nFeed*,*o* − *nFeed*) converted feed of glycerol; *zi* and *zFeed* represent the number of carbon atoms in molecule of product *i* an in the feed of glycerol. The calculated selectivities are therefore carbon-based values. The products of the dehydration of glycerol and/or the catalytic transformation of 3-HPA and of acetol were identified by GC/MS (Varian 3800; OPTIMAWAX, 30 m) coupled with a 1200 TQ mass spectrometer.

3. Result and discussions

3.1. Textural properties

The XRD patterns of commercial Al_2O_3 and TiO_2 impregnated with H_3PO_4 are presented in Fig. 1. The impregnated Al_2O_3–PO_4 cal-

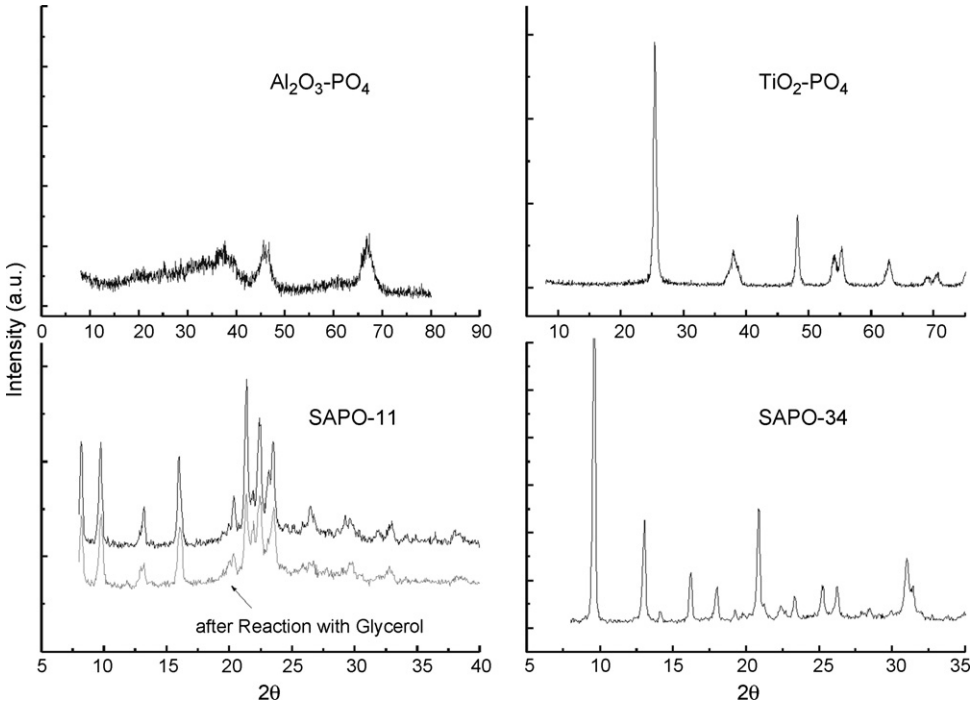

Fig. 1. XRD patterns of SAPO-11 and SAPO-34samples and Al_2O_3–PO_4 and TiO_2–PO_4 samples calcined at 530 °C and for SAPO-11 additionally after dehydration of glycerol at 280 °C for 10 h.

Table 1
Texture properties and results from NH_3-TPD measurements.

Catalyst	A_{BET} (m^2/g)	Average pore diameter (Å)	TPD-NH_3-acidity	
			Total (μmol NH_3/g)	Intrinsic (μmol NH_3/m^2)
Al_2O_3	256	124	157	0.61
Al_2O_3–PO_4	207	111	295	1.43
TiO_2	100	147	112	1.12
TiO_2– PO_4	72	101	258	3.59
SAPO-11	89	5.9	500	5.62
SAPO-34	359	4.8	1335	3.72

cined at 550 °C showed a very broad reflection in the 2θ range from 15° to 40°. This is typical for an amorphous phase, as Al_2O_3–PO_4 coverts to a crystalline state only at 1073 °C [13]. The XRD pattern of TiO_2–PO_4 indicates that TiO_2 is anatase (cf. Fig. 1). No peaks assignable to metal phosphates were observed, suggesting a high dispersion of the acidic PO_4 groups. The XRD patterns of the two silicoaluminiumphospate samples (cf. Fig. 1) are in agreement with those of SAPO-34 and SAPO-11 reported in the literature [14].

The BET surface areas and the average pore diameters are presented in Table 1 together with the total acidity of the catalysts. The surface areas of TiO_2–PO_4 and Al_2O_3–PO_4 samples were between 70 and 200 m^2/g. A decrease in the average pore diameter and in the surface area due to the phosphate promotion was observed. Obviously, the PO_4 groups blocked some of the pores, thus, lowering the available surface area.

3.2. Catalyst acidity

The NH_3 TPD profiles of the fresh samples are presented in Fig. 2. According to Tanabe et al. [15] the strength of solid acid sites within TPD profiles can be classified by the temperature of desorption of NH_3 as weak (120–300 °C), moderate (300–500 °C) and strong (500–650 °C). However, such classification is relative and especially in the case of zeolites (H-form) and SAPO materials the temperature of NH_3 desorption between 350 and 450 °C is considered as strong acidity. The Al_2O_3 support calcined at 530 °C showed as expected a much higher total acidity (μmol/g) than TiO_2. Impregnation of Al_2O_3 and TiO_2 (not shown) with H_3PO_4 induces new weak and moderate acid sites. The deconvolution of the TPD profiles of Al_2O_3–PO_4 and TiO_2–PO_4 into weak, moderate and strong Brønsted and Lewis acid sites was difficult, since the profiles strongly overlapped. Therefore, the surface acidity was calculated as total acidity and expressed per μmol of NH_3 desorbed per gram of catalyst, between 100 and 600 °C. Additionally,

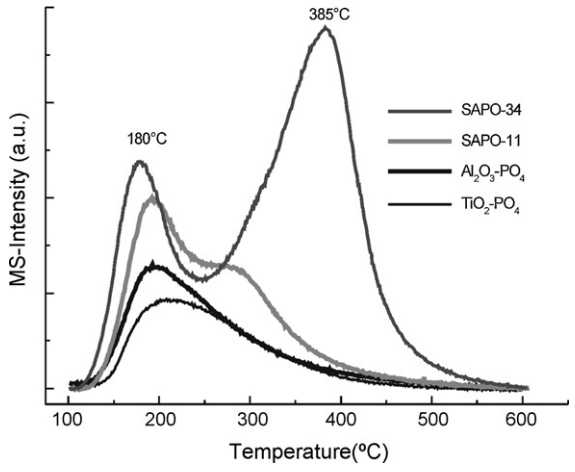

Fig. 2. NH_3-TPD profiles of SAPO-11 and SAPO-34 samples and of Al_2O_3–PO_4 and TiO_2–PO_4 samples.

the acidity is given as μmol of NH_3 per m^2 of surface area (cf. Table 1).

TPD of NH_3 of SAPO-11and SAPO-34 (cf. Fig. 2) showed two distinct peaks at low and high temperature respectively being similar to those reported by Ashtekar et al. [16]. The peaks with maxima at 185–190 °C correspond to weak acid sites from surface hydroxyl groups. The peaks with maxima at 290 and 385 °C correspond possibly to Brønsted acid sites of moderate and strong acidity of SAPO-11 and SAPO-34 respectively. The amount of moderate and strong acid sites is the highest for SAPO-34. The observed acidity of the SAPO samples is of the same order as that reported by Schnabel et al. [17]. Fig. 2 clearly shows that the SAPO-34 and SAPO-11 samples have higher acidity than the Al_2O_3–PO_4 and TiO_2–PO_4 samples.

3.3. Catalytic activities

As stated in many publications [2–6], a GHSW (space velocity) of glycerol of about 20–100 h^{-1} and temperatures in the range of 280–310 °C are the best conditions for the conversion of glycerol to acrolein over acidic catalysts such as H-ZSM5, supported heteropolyacids, aluminophosphates and solid phosphoric acid. Consequently, we performed several tests with selected catalysts at 280 °C and space velocities close to 43 and 90 h^{-1}. Pure alumina and titania (Al_2O_3 and TiO_2) supports with low acidity showed only very low conversion of glycerol (10–15%) at 280 °C. Therefore, they are not further discussed in this paper. As shown in Fig. 3, a decrease in conversion with the reaction time over all tested catalysts was observed in the catalytic dehydration of glycerol. The deactivation phenomenon can be explained by the formation of coke. This effect was more pronounced for SAPO-34 which is due to the high total acidity of the sample and its narrow pores. In the case of Al_2O_3–PO_4, the decrease in the glycerol conversion was very slow. The lower rate of deactivation in this case was likely due to larger pores and the lower acidity in comparison to the SAPO catalysts. The TiO_2–PO_4 sample deactivated much faster, despite size of the pores similar to the alumina phosphate catalysts. The explanation of this fact might be the lower surface area and correspondingly a higher intrinsic acidity leading to higher coke formation in case of the TiO_2–PO_4 sample. The effect of total acidity on the product distribution after 1 h time on stream is shown in Table 2. In addition to the desirable acrolein which is the main product resulting from double dehydration of glycerol, acetol appeared as the main by-product as a result of mono dehydration. Other detected by-products were acetaldehyde, acetone, propionaldehyde, and allyl alcohol, all of them with selectivity usually below 2–5%.

It is important to emphasize that the comparison of conversion and selectivity between different catalysts is possible only at low times on stream since with increasing time of reaction, the deactivation process becomes predominant. The results, given in Table 2 show that at constant reaction conditions the selectivity to acrolein increased with increasing total acidity of catalysts. The highest selectivity to acrolein of 62–72% was obtained on the SAPO samples. The lower conversion can be explained by an abrupt deactivation already after 60 min, because of much higher acidity of SAPO cata-

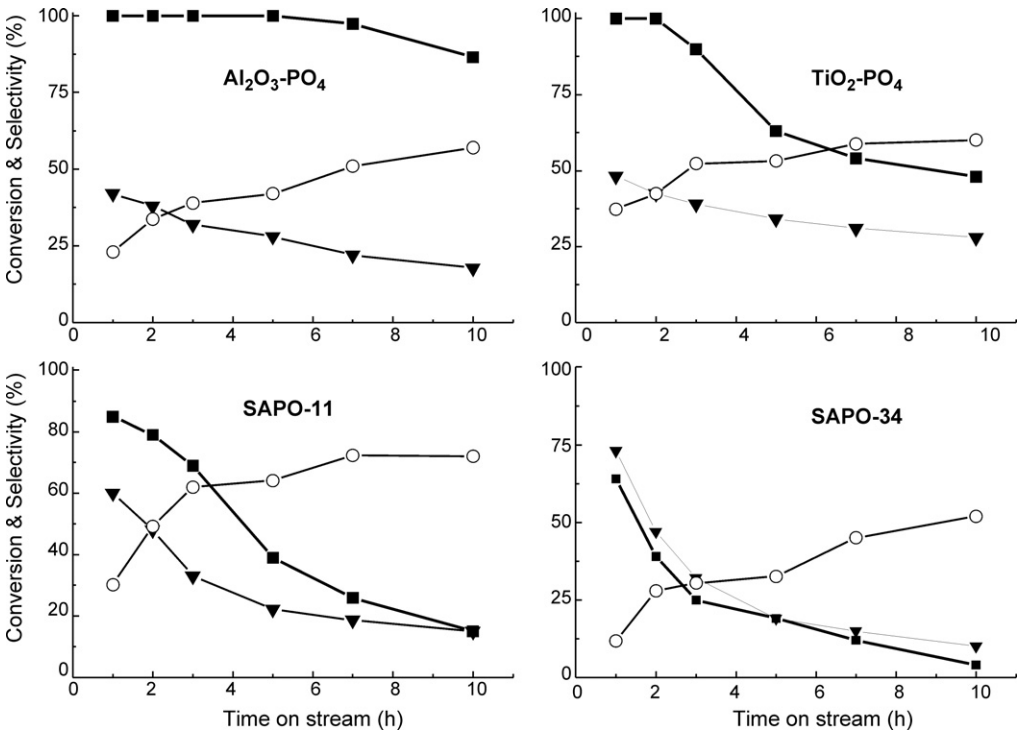

Fig. 3. The conversion of glycerol (■) the selectivity to acrolein (▼) and to acetol (○) over different acidic catalysts is shown as a function of time on stream. Reactions conditions: *T*: 280 °C, GHSV: 43 h^{-1}.

lysts. The acetaldehyde, propionaldehyde and acetone selectivities increased also with increasing catalyst acidity, while the selectivities to acetol and allyl alcohol decreased slightly. Traces of glycidol and 3-HPA were detected with selectivities around 2–3%. The formation of these intermediates was proposed by computational studies and identified by MS analysis during thermal dehydration of glycerol [18]. When the space velocity was increased to 90 h^{-1} (decreasing the residence time) glycerol conversion and selectivity towards acrolein decreased in all cases as shown in Table 2. At the same time, an increase in the formation of acetol was observed (not shown in Table 2), whereas coke yields and selectivity to carbon monoxide decreased significantly. This demonstrates that acetol is a primary but unstable product and that acetone and allyl alcohol are secondary products. In addition a formation of furan derivates was detected, suggesting, that other minor products besides acetol and 3-HPA were formed from glycerol. The formation of phenol with a selectivity of about 8–10% at low TOS (1–2 h) was only observed over SAPO-11 and Al_2O_3–PO_4. After 3–5 h TOS the selectivity to phenol dropped to ca. 1%. Phenol was also detected by Dubois et al. [3] during the dehydration of glycerol at 300 °C over WO_3–ZrO_2, ZrO_2–SO_4 and Al_2O_3–PO_4 catalysts. Phenol was probably formed from a dimerisation–cyclisation reaction of glycerol followed by a consecutive dehydration and/or from acrolein and acetone via a Diels-Alder reaction over acidic sites [19]. The possible formation of furan derivates will be discussed in the next sections. A large amount of other compounds (23–35%) remained

Table 2
Product selectivity during the catalytic dehydration of glycerol over acidic catalysts at different space velocities obtained after 60 min TOS.

	Catalyst			
	Al_2O_3–PO_4	TiO_2–PO_4	SAPO-11	SAPO-34
Total acidity (μmol NH_3/g)[a]	170 (295)	150 (258)	125 (500)	280 (1335)
Glycerol conversion (%) at GHSV 43 and 90 h^{-1} [b]	100 (74)	98 (70)	88 (65)	59 (42)
Molar carbon selectivity (%)[c]				
Carbon monoxide	1.6	2.1	2.8	3.4
Acetaldehyde	2.9	2.3	4.5	4.8
Acetone	1.7	2.0	2.2	5.0
Acrolein	42 (38)	37 (34)	62 (55)	72 (65)
Acetol	23	30	10	6.8
Allyl alcohol	2.4	2.8	1.5	2.0
Propionaldehyde	1.6	1.7	2.5	1.9
Phenol	12	0.0	8.2	0.0
Glycidol	1.2	1.5	1.0	1.2
Other products[d]	11	17	5.6	2
Coke deposit (wt% of C)	1.8	4.1	5.4	6.6

Reactions conditions: *T*: 280 °C; Feed: 600 mg/h aqueous solution of 5 wt% glycerol. Helium flow: 100 ml/min.

[a] Total acidity of used catalysts after reaction at 280 °C for 10 h and of fresh calcined catalysts (values in brackets).

[b] GHSV calculated according to the glycerol stream.

[c] The values in brackets corresponded to a GHSV of 90 h^{-1} (with respect to glycerol).

[d] Selectivity for other = 100% minus total selectivity for all products identified.

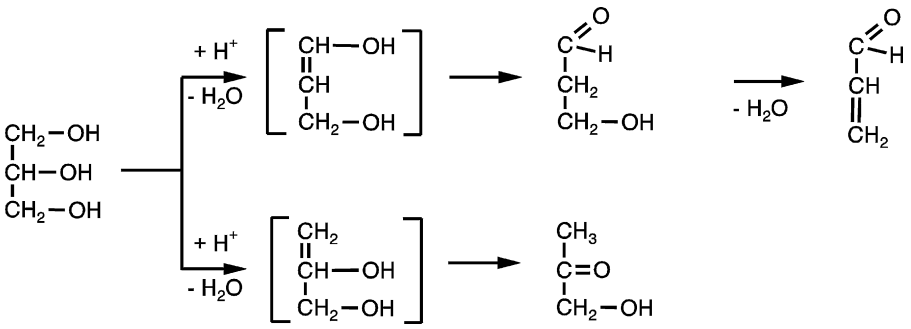

Fig. 4. Schematic representation of the dehydration of glycerol to acrolein and acetol.

unidentified (not determined by GC analysis, but calculated from the carbon-balance). They were possibly formed by secondary reactions between products or between products and the glycerol feed.

3.4. Conversion of 3-hydroxypropionaldehyde

The dehydration of glycerol proceeds in two parallel reaction pathways. Formation of acrolein and acetol is initiated by dehydration involving protonation of either secondary or primary OH-groups [7]. This leads to the formation of two different types of enol intermediates (Fig. 4). These enols undergo rapid rearrangement to acetol and to 3-HPA respectively. The 3-HPA is a very reactive hydroxyl carbonyl compound [12] which can easily give rise to a second dehydration resulting in the valuable product, i.e., acrolein. In order to investigate the main pathway, a water solution of 3-HPA was introduced into the reactor at 280 °C. The results are shown in Table 3 (at similar operation conditions as for the dehydration of glycerol). A conversion of 100% of 3-HPA was obtained for all catalysts. This indicates that 3-HPA is more easily decomposed and shows a higher selectivity to acrolein, in comparison to that obtained by the dehydration of glycerol. Additionally, CO, formaldehyde, acetaldehyde and significant amounts of coke were formed from 3-HPA (cf. Table 3). The coke, formaldehyde and acetaldehyde formation was substantially higher on the SAPO catalysts than on Al_2O_3–PO_4 and TiO_2–PO_4. Tsukuda et al. [4] and Chai et al. [5] proposed that the decomposition of 3-HPA should yield acetaldehyde and formaldehyde by a retro aldol condensation. Additionally, formaldehyde may also be decomposed to carbon monoxide and hydrogen. Besides those cleavage products, some cyclic C_6-compounds and 3,4-dihydro-1,2-pyran-2-carboxaldehyde were identified by GC/MS (cf. Fig. 5).

Also dioxolanes I and II (cf. Fig. 5) were identified in the reaction products during the catalytic dehydration of glycerol over Al_2O_3–PO_4 and TiO_2–PO_4 catalysts. They may be formed in two ways: (i) via acid-based catalytic oligomerisation of glycerol [20] or (ii) via a dimerisation of 3-HPA. Interestingly, during the dehydration of glycerol and the conversion of 3-HPA over SAPO-11 and SAPO-34 only traces of C_6 cyclic derivates were found. This indicates that the formation of C_6 cyclic compounds proceeds only in the large pore catalysts (Al_2O_3–PO_4 and TiO_2–PO_4). This can be considered as a shape selectivity effect.

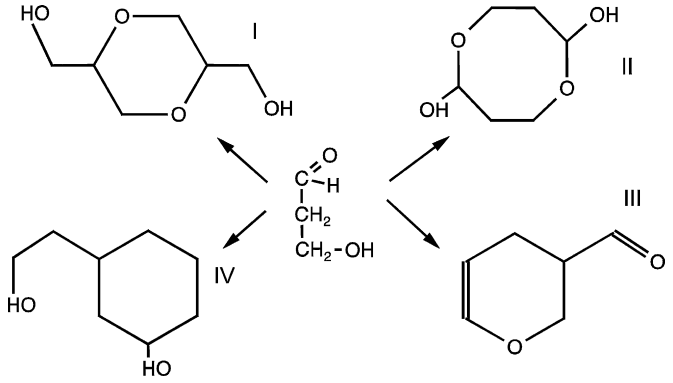

Fig. 5. Cyclic C_6 derivates identified by GC/MS-analysis during catalytic conversion of 3-hydroxy-propionaldehyde over Al_2O_3–PO_4.

3.5. Conversion of 1-hydroxyacetone

The decomposition of acetol (*1-hydroxyacetone*) was also investigated. An acetol–water solution was introduced into the reactor over acidic catalysts at 280 °C. The results presented in Table 4 show that at 280 °C acetol was more reactive on both SAPO catalysts than on Al_2O_3–PO_4 and TiO_2–PO_4 with conversions of 32–38%

Table 3
Product selectivity of catalytic conversion of 3-hydroxypropionaldehyde (3-HPA) over acidic catalysts.

	Catalyst			
	Al_2O_3–PO_4	TiO_2–PO_4	SAPO-11	SAPO-34
3-HPA conversion (%)	100	100	100	100
Molar carbon selectivity (%)				
Carbon monoxide	2.2	2.5	10	12
Acrolein	67	67	87	85
Acrolein dimers[a]	13	14	1,1	1,5
Sum of cyclic compounds[b]	18	16	<0.5	<0.5
Coke deposit (wt% of C)	12	14	33	39

Reactions conditions: *T*: 280 °C; GHSV: 43 h^{-1}; feed: 600 mg/h aqueous solution of 5 wt% 3-HPA. Helium flow: 100 ml/min, catalyst: 200 mg.

[a] 3,4-Dihydro-1,2-pyran-2-carboxaldehyde.

[b] For the structures of cyclic compounds see Fig. 5.

Table 4
Product selectivity of catalytic conversion of 1-hydroxyacetone (acetol) over acidic catalysts.

	Catalyst			
	Al_2O_3–PO_4	TiO_2–PO_4	SAPO-11	SAPO-34
Acetol conversion (%)	21	17	32	38
Molar carbon selectivity (%)				
Carbon monoxide	2.2	2.5	5.6	6.3
Acetaldehyde	3.8	3.7	7.3	6.2
Acetone	5	4.5	7.3	7.2
Propionaldehyde	2	1.5	3.8	4
Acetic acid	3.2	3	4.5	5.3
Propionic Acid	1.9	2	3.5	6.2
Sum of furane derivates[a]	35	38	20	18
Other	25	27	18	12
Coke (wt% of Carbon)	21	18	29	33

Reactions conditions: *T*: 280 °C; GHSV: 43 h^{-1}; feed: 600 mg/h aqueous solution of 5 wt% acetol. Helium flow: 100 ml/min; catalyst: 200 mg.

[a] For the structures of these compounds see Fig. 6.

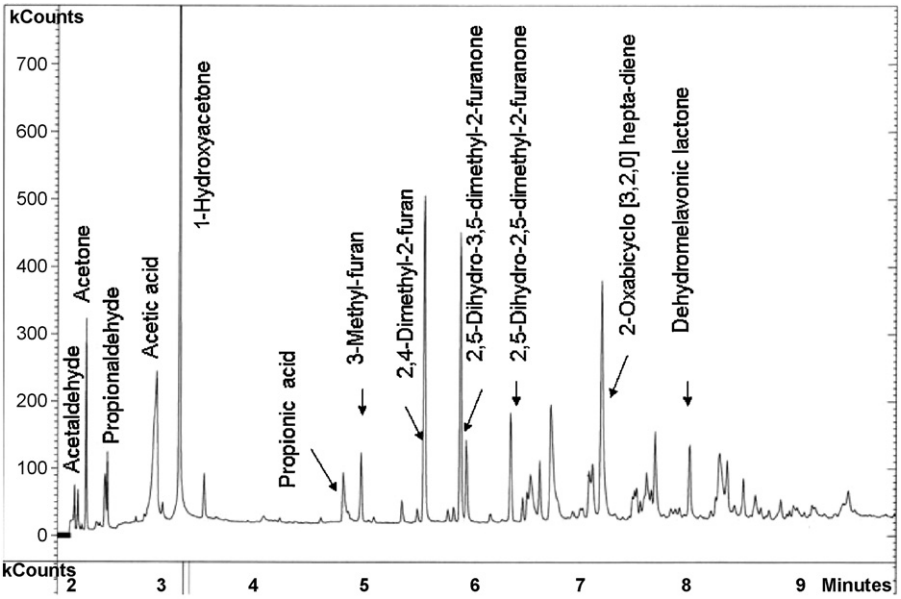

Fig. 6. GC chromatogram obtained after conversion of acetol over Al_2O_3–PO_4.

and 17–21% respectively. But acetol was found to be much less reactive than glycerol or 3-HPA. Fig. 6 shows a GC chromatogram obtained after the reaction of acetol over Al_2O_3–PO_4 at 280 °C. Acetaldehyde, acetone and acetic acid can be obtained from the catalytic C–C bond cleavage of acetol [21,22]. Propionic acid can be formed via rearrangement of acetol [23] (cf. Fig. 7). Various furan derivatives are the result of a catalytic cyclisation of acetol (cf. Fig. 8). Coke deposits were formed on the acid sites of the catalysts by secondary condensations of C_2-, C_3-aldehydes and/or furan derivatives, via an acidic mechanism. In the case of SAPO-11 and SAPO-34, which possess a narrow pore size and high acidity, the yield of acetaldehyde, propionaldehyde and acetic acid was 2–3 times higher than over TiO_2–PO_4 and Al_2O_3–PO_4 and the amount of dimerisation/cyclisation products was almost two times lower.

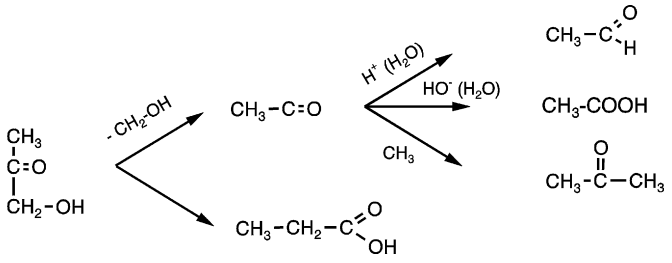

Fig. 7. Formation of carbonyl compounds via cleavage and isomerization of acetol.

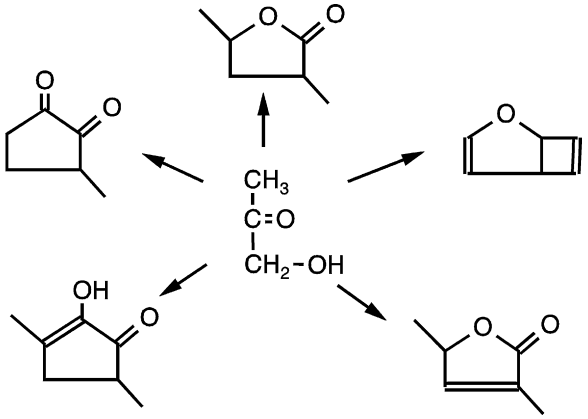

Fig. 8. Retro aldol dimerisation (cyclisation) of acetol to furan derivates.

3.6. Characterization of used catalysts

SAPO-11, SAPO-34, Al_2O_3–PO_4 and TiO_2–PO_4 catalysts deactivated already after a few hours. The deactivation of catalysts may occur due to the dissolution of active acidic sites and/or by blocking the surface by carbonaceous deposits. To understand the cause of deactivation during dehydration of glycerol, changes in the chemical properties of used catalysts and the nature of coke deposits were investigated. XRD investigations of the used SAPO-11 catalyst, showed no signals for graphitic carbon, suggesting that the carbon deposits existed as amorphous carbon species on the catalyst surface (cf. Fig. 1).

The acidic properties of the catalysts were studied after 5 h and 10 h TOS of glycerol dehydration at standard reaction conditions (280 °C; 200 mg catalyst; liquid flow 600 mg/h of 5 wt% aqueous solution of glycerol). Few changes in the total acidity of SAPO catalysts were observed after dehydration reaction. The treatment with the reaction mixture resulted in a strong decrease in total acidity of SAPO-34 sample (−82%) as shown in Table 5. In contrast, Al_2O_3–PO_4 and TiO_2–PO_4 samples exhibited only slight decrease (15–25%).

Additionally, the influence of water on the change of textural properties and the acidity of the catalysts was investigated. The catalysts were treated with water under reaction conditions similar to that of the dehydration of glycerol. The total loading of the catalysts with water was 16 g water per 1 g catalyst for 10 h. At 300 °C a moderate increase in acidity of the weak acid sites was observed (cf. Fig. 9). This suggests that after treatment with water some extra-framework alumina species such as $Al(OH)_2^+$ and $Al(OH)^{2+}$ and titania species are formed which are weak Lewis acid sites [24].

3.7. Characterization of carbon deposits

Considerable amounts of carbon deposits were formed on the catalysts during the catalytic reaction. The formation of carbonaceous deposits or coke is an undesired side reaction for almost all reactions of hydrocarbons and alcohols over acidic catalysts. Reaction conditions, especially the reaction temperature and the kind

Table 5
Acidity, surface areas, and coke loadings of the used catalysts after dehydration of glycerol at different reactions temperature in comparison to the fresh catalysts (values in squared brackets).

	Al_2O_3–PO_4	TiO_2–PO_4	SAPO-11	SAPO-34
Total acidity (μmol NH_3/g)	170 [295]	150 [258]	280 [1330]	125 [498]
S_{BET} (m^2/g)	206 [118]	72 [38]	359 [172]	89 [49]
Coke loading wt% of Carbon[a] and H/C ratio[b]				
280	2.4 (0.54)	3.1 (0.55)	4.6 (0.66)	9.6 (0.62)
300	3.9 (0.52)	6.8 (0.50)	7.4 (0.55)	12.7 (0.54)
320	5.8 (0.49)	8.9 (0.48)	9.5 (0.49)	16.2 (0.47)

Reaction conditions: feed: 600 mg/h aqueous solution of 5 wt% glycerol, GHSV: 90 h^{-1}.
[a] Results of elemental analysis.
[b] Values in brackets correspond to H/C ratios.

of reactant feed, have a great influence on coking during catalysis on acidic catalysts [25,26]. The nature of the support plays also an important role in coking. Table 5 shows the amount of coke accumulated on the catalysts after reaction at different temperatures. At 280 °C, the coke loadings are the highest (>9%) for the most acidic catalyst SAPO-34. This is comparable to the coke values found for a strongly acidic Nb_2O_5 catalyst [8]. A lower coke deposition was found for SAPO-11 and even much lower coke loadings were detected on Al_2O_3–PO_4 and TiO_2–PO_4 due to their lower total acidity. At 300 and 320 °C the amounts of coke deposits were higher for all catalysts. The H/C ratios of the carbonaceous deposits formed at 280 °C on TiO_2–PO_4 and Al_2O_3–PO_4 lie at 0.54–0.55, whereas the H/C ratio for the SAPO samples were considerably higher (0.62–0.66). The large difference in the amount of coke deposits and in the H/C ratios at 280 °C appears to correlate with the total acidity and effective pore widths of the catalysts. At higher reaction temperatures, the carbonaceous deposits are getting more deficient in hydrogen, indicating that highly condensed, unsaturated and polynuclear aromatic deposits are formed.

3.8. Temperature programmed combustion of coke deposits

TPO characterization of the used catalysts (after 7 h TOS) was performed using an air flow in the DTA/TG mode. Fig. 10 shows the formation of carbon dioxide during the temperature programmed combustion of coke deposits after reaction at 280 °C for 10 h. The CO_2 formation curves for the Al_2O_3–PO_4 and TiO_2–PO_4 catalysts show a clear peak at lower temperatures with maxima at 317 and 365 °C, respectively. The TPO-CO_2 profiles for SAPO-11 and SAPO-34 are similar and are shifted to higher temperatures with maxima at about 500 and 540 °C, respectively. From the CO_2 profiles it is clear that on SAPO-34 more carbon is deposited than on SAPO-11.

A scheme of the formation of reaction products and of coke during the dehydration of glycerol is shown in Fig. 11.

Fig. 11 implies that the formation of amorphous carbon deposits on acidic catalysts during the dehydration of glycerol may result from consecutive reactions of glycerol (acidic catalytic oligomerisation on catalyst surface) and/or side reaction between product molecules such as acrolein, acetaldehyde, acetol (aldol condensation of carbonyl compounds), polycondensation of phenol with formaldehyde and/or acetaldehyde (formation of phenol-formaldehyde/acetaldehyde resins) and catalysed polymerisation of acrolein on acid sites. At low reaction temperatures, carbonaceous deposit may consist mainly of adsorbed high boiling products

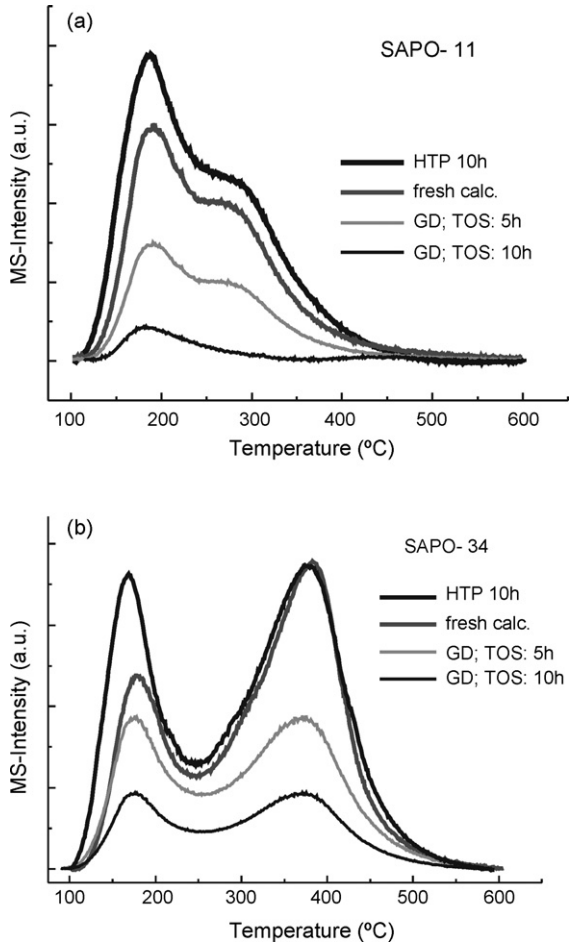

Fig. 9. NH_3 TPD profiles for SAPO-11 (a) and SAPO-34 (b) samples after calcination, hydrothermal treatment at 300 °C (HTP at 300 °C for 10 h), and after dehydration of glycerol (GD) at 280 °C for 5 and 10 h.

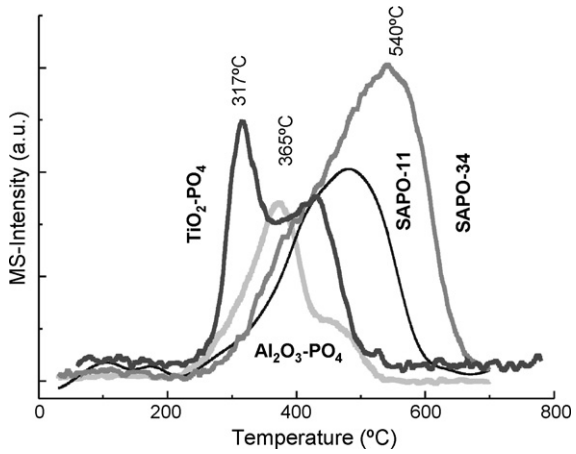

Fig. 10. Carbon dioxide desorption profiles during temperature programmed oxidation of carbonaceous deposited on used catalyst. Heating rate: 10 K min^{-1}; air flow: 75 ml/min.

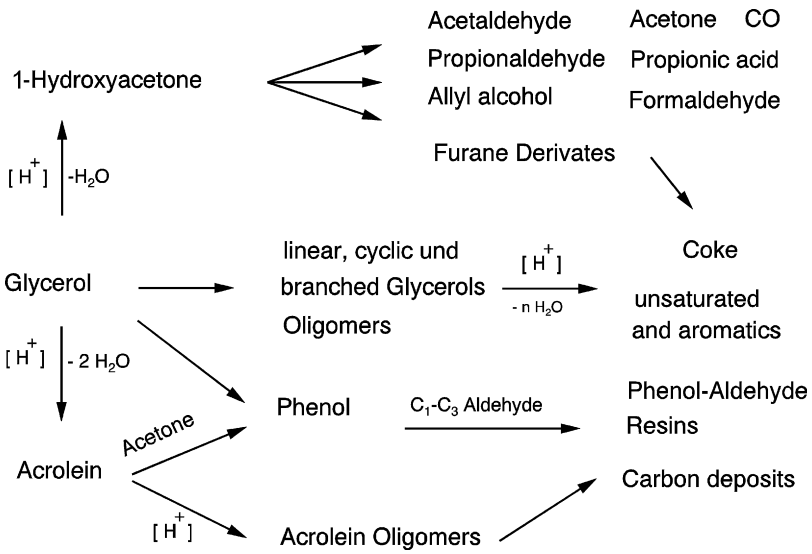

Fig. 11. General reaction scheme of the dehydration of glycerol.

(glycerol olygomers, aldol condensation products). At higher temperatures (above 300 °C) and in presence of strong acid sites the oxygenates may undergo further dehydration and condensation yielding unsaturated and aromatic compounds as well as CO_x [23]. A deactivation of $AlPO_4$ catalysts and the formation of carbonaceous deposits has already been observed during the dehydration of 1-BuOH [27].

4. Conclusions

Supported Al_2O_3 and TiO_2 phosphates and SAPOs showed a different activity in the catalytic dehydration of glycerol as well as different conversions of 2-hydroxyacetone and 3-hydroxypropionaldehyde in the presence of water. The total acidity, the texture of the supported phosphates and the reaction temperature strongly influenced both the conversion and the distribution of products. The mesoporous Al_2O_3–PO_4 and TiO_2–PO_4 catalysts with large pores exhibited high activity but limited selectivity towards acrolein. On the other hand, SAPO-11 and SAPO-34 catalysts with small micropores (5–6 Å) were less active but more selective. The small pores of SAPO catalysts favour an external surface reaction rather than a reaction inside the channels, thus, lowering activity and accelerating deactivation. Al_2O_3–PO_4 and TiO_2–PO_4 catalysts possess much larger pores; therefore, the whole surface was available for the reaction for a much longer period of time.

The comparison of the formation of acrolein and acetol over SAPO-11 and SAPO-34 catalysts showed that the pore size and nature of acidity had at low TOS a significant effect on the selectivity towards acrolein. Tsukuda et al. [4] found also that the size of pores of silica loaded with heteropolyacids had a strong influence on the performance of acidic catalysts during the dehydration of alcohols.

The amount and distribution of decomposition products observed in the reaction of 3-HPA and acetol were also strongly dependent on the texture and acidity of the catalysts. With an increase of the intrinsic acidity and the reaction temperature an increase in the amount of decomposition products was observed.

The experimental data showed that in the presence of acidic catalysts acetol was stable until 240 °C, whereas 3-HPA was already dehydrated to acrolein and condensated to cyclic C_6 compounds at 120 °C. Deactivation was observed for all acidic catalysts, but an oxidative treatment with air at temperatures around 450 °C was found to be sufficient to regenerate the deactivated catalysts and to recover acidity and activity. Our studies allow understanding the possible mechanism of the dehydration of glycerol, laying the basis for an effective regeneration of deactivated catalysts. Further investigations regarding the modification of acidic catalysts for the dehydration of glycerol, the nature of coke deposits as well as the regeneration of deactivated catalysts is in progress.

References

[1] A. Behr, J. Eilting, K. Irawaldi, J. Leschinski, F. Lindner, Green Chem. 10 (2008) 13.
[2] T. Haas, D. Arntz, H. Klenk, W. Girke, Production of acrolein from glycerol, Pat. EP. 19,930,116,792 (1994).
[3] J.-L. Dubois, C. Duquenne, W. Hölderich, J. Kervenal, Process for dehydration glycerol to acrolein, Pat. WO 2006/087084 A2 (2006).
[4] E. Tsukuda, S. Sato, R. Takahashi, T. Sodesawa, Catal. Commun. 8 (9) (2007) 1349.
[5] S. Chai, H. Wang, Y. Liang, B. Xu, Green Chem. 9 (2007) 1130.
[6] H. Atia, U. Ambruster, A. Martin, J. Catal. 258 (2008) 71.
[7] M.J. Antal, W.S.L. Mok, J.C. Roy, A.T. Raissi, J. Analyt. Appl. Pyrol. 8 (1985) 291.
[8] S.H. Cahi, H.P. Wang, Y. Liang, B.Q. Xu, J. Catal. 250 (2007) 342.
[9] H. Redlingshöfer, C. Weckbecker, K. Huthmacher, A. Dörflein, Method for regenerating a catalyst for dehydrating of glycerine, Pat. WO/2008/092534 (2008).
[10] K.M. Parida, T. Mishra, S.B. Rao, Appl. Catal. A: Gen. 166 (1998) 115.
[11] B.M. Lok, C.A. Messnia, R.L. Patton, R.T. Gajek, T.R. Cannan, E.E. Flanigen, J. Am. Chem. Soc. 106 (1984) 6092.
[12] R.H. Hall, E.S. Stern, J. Chem. Soc. (1950) 490.
[13] K.M. Parida, T. Mishra, J. Colloid Interf. Sci. 179 (1996) 233.
[14] B.M. Lok, C.A. Messina, R.L. Patton, R.T. Gajek, Patent USA 4.440.871 (1984).
[15] K. Tanabe, M. Misono, Y. Ono, H. Hattori, New solid acids and bases: their catalytic properties, Stud. Surf. Sci. Catal. 51 (1989) 5–25.
[16] S.S. Asthekar, V.V. Chilukari, D.K. Charkabarty, J. Phys. Chem. 98 (1994) 4878.
[17] K.H. Schnabel, R. Fricke, I. Girnus, E. Jahn, E. Löffler, B. Paraliz, J. Chem. Soc. Faraday Trans. 87 (1991) 3574.
[18] M.R. Nimlos, S. Blanskby, X. Qian, M.E. Himmel, D.K. Jonson, J. Phys. Chem. A 110 (2006) 6145.
[19] B.N. Dolgov, T.V. Nizovkina, L.V. Mozhukhin, Zh. Obshch. Khim. 22 (1952) 950.
[20] J. Barrault, Y. Pouilloux, J.M. Clacens, C. Vanhove, S. Bancquart, Catal. Today 75 (2002) 177.
[21] A. Corma, B.W. Wojciechowski, Catal. Rev. 27 (1985) 29.
[22] A. Corma, P.J. Miguel, A.V. Orchilles, J. Catal. 145 (1994) 171.
[23] A. Corma, W.H. Huber, L. Sauvanaud, P. O'Connor, J. Catal. 257 (2008) 163.
[24] F. Lonyi, J. Valyon, Microporous Mesoporous Mater. 47 (2001) 293.
[25] J. Kijenski, A. Migdal, O. Osawaru, E. Smigiera, Pat. PL 37928306 (2006).
[26] M. Neuber, S. Ernst, H. Geerts, P.-J. Grobet, P.A. Jacobs, G.T. Kokotailo, J. Weitkamp, Stud. Surf. Sci. Catal. 34 (1987) 567.
[27] F.M. Bautista, B. Delmon, Appl. Catal. A: Gen. 130 (1995) 47.